RSC Advances

Proposed correlation of glass formation ability with critical dosage

for the amorphous alloys formed by ion beam mixing

M.H. Yang, J.H. Li[*] and B.X. Liu

Key Laboratory of Advanced Materials (MOE), School of Materials science and

Engineering, Tsinghua University, Beijing 100084, China

ABSTRACT

A negative correlation of glass formation ability with the critical dosage, i.e.
minimum ion-dosage, is first proposed for the amorphous alloys formed by ion beam
mixing (IBM), i.e. the lower the critical ion-dosage (D_c) the better the glass formation
ability (GFA), suggesting that D_c could serves as an indicator to GFA of these alloys.
The correlation is not only supported by the results of experiments such as IBM and
liquid melt quenching (LMQ), but also is proven to be relevant by thermodynamic
calculations. The proposal helps to bridge the gap of experimental data between
different producing methods, e.g. making it possible to apply the IBM results to
designing the alloy composition in producing metallic glasses by LMQ. The limitation
and prospect are also presented in discussion.

Keywords: Amorphous alloys; Glass formation ability; Critical ion-dosage; Ion
beam mixing

---

[*] Corresponding author: lijiahao@mail.tsinghua.edu.cn.

Due to the excellent mechanical, chemical and physical properties, the amorphous alloys, i.e. metallic glasses, have been attracting a great of attentions as a prominent class of functional and structure materials [1-2]. To date, a great number of binary, ternary and even multicomponent amorphous alloys have been obtained through a variety of powerful producing techniques, such as liquid melt quenching (LMQ), ion beam mixing (IBM), and mechanical alloying (MA) [3-4]. In order to facilitate the production of amorphous alloys, one of the basic issues is to search for an appropriate method or parameter to indicate the glass-formation ability (GFA) that describes the easiness or difficulty of metallic glass formation. In principle, GFA not only depends on the applied producing techniques, but is also governed by the intrinsic characteristics of the system. In practice, the GFA is evaluated usually by the maximum size (D_{max}) of the obtainable metallic glasses, or the minimum cooling speed (R_c) to produce metallic glasses by LMQ, e.g. copper model casting [5]. The smaller R_c or the larger D_{max} is, the better GFA of the alloy should be. However, there is still lack of a proper parameter to describe the GFA of those amorphous alloys formed by IBM. The present work attempts to solve this problem by correlating the GFA of those amorphous alloys with the dosage of IBM.

Ion beam mixing is a process of far-from equilibrium and is commonly divided into three steps, i.e. the atomic collision cascade, relaxation and delayed period. Generally, the first and second steps are of importance in determining the structural characteristics of the alloy phases, however, the last step has no considerable effect on the structure of alloys. In the first step, when an ion, with the energy higher than a

critical value, impacts on the surface and penetrates into the multilayered films, an atomic collision cascade will be triggered, i.e. the impinging ion knocks out an atom from its own site and the knocked-out atom, if its energy is still high enough, will result in secondary collision, third collision, and so on and so forth. The atoms are excited into such violent motion by the impinging ions and knocked-out atoms that not only the crystalline lattices are destroyed but also the interface of multilayered film are smeared out, thus obtaining a highly disordered atomic mixture. Apparently, the uniform mixing is induced by dynamic collision process together with the associated irradiation enhanced diffusion. In the relaxation step, the highly energetic mixture should somehow relax towards equilibrium. However, whether or not the mixture can reach an equilibrium state depends on the kinetics conditions available in IBM [6]. An alternatively way of examining the process of ion irradiation is to consider the energy deposition in the surface of the target material and a concept of thermal spike was introduced. As radiation defects created in materials by highly energetic ions are cylindrical, a time-dependent thermal transient process is expressed in cylindrical geometry:

$$\rho C_e(T_e)\frac{\delta T_e}{\delta t} = \frac{\delta}{\delta r}\left[K_e(T_e)\frac{\delta T_e}{\delta r}\right] + \frac{K_e(T_e)}{r}\frac{\delta T_e}{\delta r} - g(T_e - T) + A(r) \tag{1}$$

$$\rho C(T)\frac{\delta T}{\delta t} = \frac{\delta}{\delta r}\left[K(T)\frac{\delta T}{\delta r}\right] + \frac{K(T)}{r}\frac{\delta T}{\delta r} - g(T - T) \tag{2}$$

where C_e, C and K_e, K are the specific heat and thermal conductivity for the electronic system and lattice, respectively, ρ is the material density, $A(r)$ is the energy brought on the electronic system in a time t considerably less than the electronic thermalization

time and r is the radius in cylindrical geometry with the heavy ion path as the axis. $A(r)$ can be defined as $\iint 2\pi r A(r,t)\mathrm{d}r\mathrm{d}t = S_e$. The electron-phonon coupling factor g is given by $g = \dfrac{\pi^4 (k_B n_e s)^2}{18 K_e(T_e)}$. Here, k_B is the Boltzmann's constant, n_e is the electron density and s is the speed of sound in the metal.

From the numerical analysis of the coupled equations, the lattice temperature $T(r, t)$ at each time t and radius r can be calculated. The maximum temperature $T_{\max}(r)$ reached by the lattice at a radius r from the ion path is dependent on the electronic stopping S_e. The temperature of electronic system increases during a time equivalent to the energy deposition time $\sim 10^{-15}$ s. Then the lattice temperature increases mainly because of the electron-phonon interaction. The maximum lattice temperature $\sim 10^4$ K is reached when both systems are in equilibrium at a mean time equal to $C_e(T_e)/g(T_e)$, which is of the order of 10^{-12} s. Above a certain S_e threshold, this lattice temperature may exceed the melting temperature T_m of the lattice within a cylinder of radius r_m, i.e. latent track, of the order of a few nm. After that time both temperatures decrease and are governed by the thermal conductivity. The molten phase is quenched with an effective cooling rate of the order of 10^{15} K/s. Such a high cooling speed makes the kinetic condition for alloy phase formation to be extremely restricted, thus allowing only peculiar phases, i.e. amorphous or simple structured crystalline alloys, to be formed. Considering ion beam induced interface amorphization to take place, when the substrate temperature is decreased lower than some critical value T_r, which is a function of implant conditions, the sign of the growth rate $V_r = -\mathrm{d}h/\mathrm{d}D$ (where h is the a-layer thickness, and D is the delivered dose) changes. This transition from the

crystallization to amorphization regime can also be caused by increasing the accelerating voltage, the beam flux F, and also dependent on irradiation conditions, such as ion species and energy, dopant type and concentration, and a/c interface orientation with respect to the crystallographic axes [7].

Based on the above explanation, it can be seen that the key factor in formation of amorphous alloys is to destroy the structure of the crystalline lattices by ion beam. The more stable, or the more difficult to destroy the crystalline lattice, the more difficult the amorphous alloys to be formed. Therefore, to obtain the amorphous alloys, more ion-dosage is required to destroy the crystalline lattice. The corresponding alloy could therefore be considered as a poor glass-former, i.e. the GFA of this alloy is also poor. It suggests that, under the same circumstance such as accelerating voltage and the beam flux, more ion-dosage is needed to produce this amorphous alloy by IBM. Naturally, if the GFA of an alloy is good, then the small ion-dosage is needed to produce this amorphous alloy. For either good or poor glass-former, it is reasonable that there is a critical ion-dosage D_c, i.e. the minimum ion-dosage, less which no uniform amorphous alloys could be obtained. However, the critical ion-dosage D_c for a good glass-former is lower than that for a poor glass-former to produce amorphous alloys. It suggests that there exists a negative correlation between the critical ion-dosage D_c and the GFA of amorphous alloys formed by IBM, i.e. the lower the critical ion-dosage D_c, the better the GFA of an alloy. To verify the relevance of this negative correlation, the IBM experiments were carried out on the Ni-Mo-(Ti, Zr) multilayered films.

In present study, the overall compositions of the Ni-Mo-(Ti, Zr) multilayered films were designed to be $Ni_{40}Mo_{20}(Ti_{1-x}Zr_x)_{40}$, x=0, 0.25, 0.50, 0.75 and 1. The thickness of a multilayered film is designed as about 40 nm to match the irradiating ion range [8]. The desired multilayered films were prepared by depositing alternatively pure Ni (99.99%), Mo (99.99%), Ti (99.99%) and Zr (99.99%) at a rate of 0.5 Å/s onto newly cleaved NaCl single crystal substrates in an e-gun evaporation system with a vacuum level of 10^{-6} Pa. The prepared multilayered films were then irradiated by 180 keV xenon ions in an implanter with a vacuum level better than 5×10^{-4} Pa and the irradiation doses were in a range from 1×10^{15} to 7×10^{15} Xe^+/cm^2. During the irradiation, the sample holder was cooled by liquid nitrogen (77 K) and the ion beam current density was confined to be about 2 μA cm^{-2} to avoid an overheating effect. The real compositions of the as-deposited multilayered films were all determined by X-ray fluorescence (XRF). The real compositions are (1) $Ni_{41}Mo_{21}Ti_{38}$, (2) $Ni_{41}Mo_{18}Ti_{31}Zr_{10}$, (3) $Ni_{39}Mo_{20}Ti_{21}Zr_{20}$, (4) $Ni_{40}Mo_{22}Ti_{10}Zr_{28}$, and (5) $Ni_{40}Mo_{22}Zr_{38}$, while the designed compositions are (1) $Ni_{40}Mo_{20}Ti_{40}$, (2) $Ni_{40}Mo_{20}Ti_{30}Zr_{10}$, (3) $Ni_{40}Mo_{20}Ti_{20}Zr_{20}$, (4) $Ni_{40}Mo_{20}Ti_{10}Zr_{30}$, and (5) $Ni_{40}Mo_{20}Zr_{40}$. It was found that there were few differences between the real compositions and the designed compositions, indicating the accuracy of the film composition controlling. For structural characterization, the Ni-Mo-(Ti, Zr) films at deposition state and upon irradiation were examined by bright field image and selected area diffraction (SAD) of transmission electron microscopy (JEM 200 CX). High-resolution transmission

electron microscopy (HRTEM) was also used for analyzing the bright field image of samples. The results of IBM experiment were summarized in Table 1.

The IBM experiment shows that amorphous alloys could be formed in the $Ni_{40}Mo_{20}(Ti_{1-x}Zr_x)_{40}$ multilayered films upon irradiation to appropriate dosages. At lower ion-dosage, the mixtures of amorphous and crystalline phases were formed, while the uniform amorphous alloys were obtained with increasing the dosage of ion beam mixing to higher values. Fig. 1(a) shows the bright field image of the $Ni_{40}Mo_{20}Ti_{10}Zr_{30}$ multilayered films upon irradiation of 1×10^{15} Xe^+/cm^2. The corresponding SAD pattern was shown in Fig 1(b), in which both the diffused halos of amorphous phases and the diffraction rings of crystalline phase could be distinguished. Upon irradiation to the dose of 3×10^{15} Xe^+/cm^2, the $Ni_{40}Mo_{20}Ti_{10}Zr_{30}$ multilayered films turned into an uniform amorphous phase. It can be seen from Fig. 1(c) that the bright field image exhibits a gray matrix of a typical amorphous configuration, which is confirmed by diffused halos, instead of diffraction rings, in the corresponding SAD pattern in Fig. 1(d). One notes that the similar results were also obtained in $Ni_{40}Mo_{20}Ti_{20}Zr_{20}$ and $Ni_{40}Mo_{20}Ti_{30}Zr_{10}$ quaternary multilayered films. Besides, Table 1 also shows that the minimum ion-dosages, i.e. critical ion-dosages D_c, to form uniform amorphous phases in the $Ni_{40}Mo_{20}(Ti_{1-x}Zr_x)_{40}$ multilayered films are different. For example, to form an uniform $Ni_{40}Mo_{20}Ti_{40}$ amorphous alloy by IBM in the present study, the ion-dosages should not be less than 7×10^{15} Xe^+/cm^2, otherwise only a mixture of amorphous and crystalline phases were obtained, i.e. the corresponding critical ion-dosage $D_c=7\times10^{15}$ Xe^+/cm^2. Similarly, the D_c of

$Ni_{40}Mo_{20}Ti_{10}Zr_{30}$, $Ni_{40}Mo_{20}Ti_{20}Zr_{20}$ and $Ni_{40}Mo_{20}Ti_{30}Zr_{10}$ are 3×10^{15} Xe^{+}/cm^{2}, while

the D_{c} of $Ni_{40}Mo_{20}Zr_{40}$ is 5×10^{15} Xe^{+}/cm^{2}. According to the above proposal that there

is a negative correlation between the D_{c} and the GFA of alloys, the GFAs of the

former three alloys are better than the latter two and the GFA of $Ni_{40}Mo_{20}Zr_{40}$ is again

better than $Ni_{40}Mo_{20}Ti_{40}$ alloy.

From a theoretical viewpoint, the GFA of an alloy not only depends on the

applied producing techniques, but also is governed by the intrinsic characteristics of

the system, and therefore the GFA could be estimated from some intrinsic properties

of the alloy. In the past, by considering the underlying insights of glass-formation, a

dozen of criteria or parameters have been developed to compute the GFA of a variety

of alloys. Among them, the most famous one is the reduced glass transition

temperature $T_{rg}=T_{g}/T_{m}$ proposed by Turnbull, where T_{g} and T_{m} stand for the glass

transition temperature and the melting point, respectively [9]. Later on, Lu et al.

confirmed that T_{rg} computed by T_{l}/T_{g} shows a better correlation with GFA than that

given by T_{g}/T_{m} for multicomponent alloy systems, where T_{l} is liquidus temperature

[10]. Typically, the T_{rg} value of the known metallic glasses varies between 0.4 and 0.7

[11]. Based on the considerations of super-cooled liquid stability against

crystallization, Inoue et al. proposed another parameter, i.e. the super-cooled liquid

region ΔT_{xg}, to indicate the GFA of an alloy [12]. It should be noted that this criterion

considers only the thermal stability of the glass that has been formed and does not

actually consider the ease with which the liquid forms the glass [13]. By combining

the T_{rg} and ΔT_{xg} to one, Lu and Liu also developed a new parameter $\gamma=T_{x}/(T_{g}+T_{l})$ to

predict the GFA of metallic glasses [5]. With the synthesis of a very large number of BMGs, a number of new parameters, for example, $\alpha = T_x/T_l$ [14], $\beta = T_x/T_g + T_g/T_l$ [14], $\delta = T_x/(T_l - T_g)$ [15], and $\gamma_m = (2T_x - T_g)/T_l$ [16] were proposed. Majority of these new parameters were derived using the characteristic temperatures such as T_g, T_x and T_l and their different combinations. Alternatively, by considering the competition of amorphous against crystalline phases and basing thermodynamic analysis, a simple parameter $\gamma^* \propto \Delta H^{\text{amor}}/(\Delta H^{\text{cryt}} - \Delta H^{\text{amor}})$ was proposed by Xia et al. to indicate the GFA of metallic glasses [17-18]. Here ΔH^{amor} and ΔH^{cryt} stand for the formation enthalpies of the amorphous and competing crystalline phases, respectively. Unlike those parameters derived from characteristic temperatures, the parameter γ^* can be obtained by simple thermodynamic calculation, e.g. using Miedema model, avoiding the complicated and time-consuming experimental tests and measurements [19]. Besides, the parameter γ^* is found to be widely accepted among the research community of metallic glasses [20]. For instance, great deals of LMQ experiments have shown a strong correlation of the parameter γ^* to the largest sizes of obtained glasses, suggesting that parameter γ^* could reasonably reflect the GFA of an alloy [21]. Since the critical ion-dosage D_c is proposed to correlate with the GFA of amorphous alloys, a correlation should also exist between the parameter γ^* and the critical ion-dosage. In order to prove the assumption, the values of parameter γ^* were computed for the $Ni_{40}Mo_{20}(Ti_{1-x}Zr_x)_{40}$ alloys and the calculated results are given in Table 1. Concerning the details of parameter γ^* and corresponding thermodynamic calculation, the readers are referred to the reference [22-23] and the appendix below.

Thermodynamic calculation indeed reveals a negative correlation between the parameter γ^* and the critical ion-dosage D_c. For example, Table 1 shows that the calculated γ^* of $Ni_{40}Mo_{20}Ti_{30}Zr_{10}$, $Ni_{40}Mo_{20}Ti_{20}Zr_{20}$ and $Ni_{40}Mo_{20}Ti_{10}Zr_{30}$ alloys are apparently larger than that of the $Ni_{40}Mo_{20}Ti_{40}$ and $Ni_{40}Mo_{20}Zr_{40}$ alloys. Not coincidentally, the critical ion-dosages D_c of the former three are 3×10^{15} Xe^+/cm^2, and pronouncedly lower than that of the latter two. Besides, since the γ^* values of $Ni_{40}Mo_{20}Ti_{30}Zr_{10}$, $Ni_{40}Mo_{20}Ti_{20}Zr_{20}$ and $Ni_{40}Mo_{20}Ti_{10}Zr_{30}$ alloys are so closed to each other, all around 3, the present study does not distinguish the difference of their critical ion-dosages. The calculated γ^* values of $Ni_{40}Mo_{20}Ti_{10}Zr_{30}$, $Ni_{40}Mo_{20}Zr_{40}$ and $Ni_{40}Mo_{20}Ti_{40}$ alloys are 3.06, 2.69 and 2.04, respectively, i.e. smaller and smaller, showing that their GFAs become poorer and poorer. This conclusion is also confirmed by the corresponding critical ion-dosages, i.e. 3×10^{15}, 5×10^{15}, 7×10^{15} Xe^+/cm^2, respectively. This correlation between the γ^* and D_c proves that the critical ion-dosage D_c is capable to sever as an indicator of the GFA of alloy, e.g. the lower the critical ion-dosage, the better the GFA of an alloy, the larger the parameter γ^* is and vise verse.

In order to further testify the relevance of the obtained conclusion, some IBM experimental data are collected and shown in Fig. 2 [24-30], in which the calculated γ^* values are also given. One can vividly see from this figure that there exists a negative correlation between the γ^* and D_c. With the incensement in critical ion-dosages, the γ^* values become smaller and smaller, both showing the corresponding GFA become poorer and poorer. The correlation between the GFA and

critical ion-dosage is not only supported by the present IBM experiments and thermodynamic calculation, but also is proven to be relevant by the results of other LMQ. It has been reported that when irradiated to a dose of 5×10^{15} Xe^+/cm^2, unique $Cu_{65}Zr_{35}$ amorphous alloy was obtained by IBM and its composition could be made into bulk metallic glass rods with 2 mm in diameter [31]. To take another example, the γ^* value and D_c for $Ni_{63}Nb_{28}Zr_9$ and $Ni_{79}Nb_{12}Zr_9$ alloy are 3.72, 0.6×10^{15} Xe^+/cm^2 and 2.93, 3×10^{15} Xe^+/cm^2, while the critical diameter D_{max} of $Ni_{63}Nb_{28}Zr_9$ and $Ni_{79}Nb_{12}Zr_9$ amorphous alloy are about 3 and 1 mm, respectively [32]. Compared to the $Ni_{79}Nb_{12}Zr_9$ alloy, the $Ni_{63}Nb_{28}Zr_9$ alloy has a lower D_c, a higher γ^* and a larger D_{max}, indicating that the alloy with lower D_c is easier to destroy the structure of the crystalline lattices upon IBM, obtaining a larger D_{max}. More importantly, this suggest that the present proposed correlation bridge the gap between IBM and LMQ experimental results, e.g. making it possible to apply the D_c to designing the alloy composition in producing metallic glasses by LMQ.

From the above discussion, it can be concluded that there is a negative correlation of GFA with the critical dosage for the amorphous alloys formed by IBM, i.e. the lower the critical ion-dosage D_c the better the GFA, suggesting that D_c could serves as an indicator to GFA of these alloys. Nevertheless, one should be aware that this correlation just holds qualitatively and approximately. In fact, extensive experimental results have shown that due to the extremely restricted kinetic condition, IBM should be executed under an appropriate condition, e.g. the samples should be retained at a relatively low temperature, the ion beam current density should be

relatively low to avoid an overheating effect, etc [6-7]. Considering the practical experimental procedures, there are some discrepancies to the proposed method. These discrepancies are thought to be based on the following three aspects: (1) the IBM experiments should be carried out under the same circumstance, such as accelerating voltage, ion beam current density and ion irradiation at relatively low temperature, (2) difficulty of precisely determining the minimum ion-doses to keep the melt amorphous without precipitation of any crystals during solidification, (3) limitation of the number of experimental results compared to the entire compositions of the systems. The first and second aspect would not affect the application of the proposed method, as the irradiation dose could be precisely controlled by adjusting the ion current under the same experimental circumstance, thus enabling researchers to trace the details of the amorphous phase formation. For the third aspect, it indicates that not all the compositions have been studied due to the scientific and application interests.

Conclusions

In summary, the critical ion-dosage, D_c, could be considered as an indicator to the glass formation ability (GFA) of the alloy formed by ion beam mixing (IBM). The correlation of the critical dosage D_c with the GFA, i.e. the lower the D_c, the better the GFA, is not only supported by the results of experiments such as IBM and liquid melt quenching (LMQ), but also proven to be relevant by thermodynamic calculations. The proposal correlation helps to bridge the gap of experimental data between different producing methods, e.g. making it possible to apply the IBM results to designing the alloy composition in producing metallic glasses by LMQ.

RSC Advances Accepted Manuscript

References

[1] A. Inoue, *Acta Mater*, 2000, 48, 279-306.

[2] Z.P. Lu, H. Bei and C.T. Liu, *Intermetallics*, 2007, 15, 618-624.

[3] A. Inoue, T. Zhang and T. Masumoto, *Mater. Trans. JIM*, 1989, 30, 965-972.

[4] H.W. Kui, A.L. Greer and D. Turnbull, *Appl. Phys. Lett.*, 1984, 45, 615-616.

[5] Z.P. Lu and C.T. Liu, *Acta Mater.*, 2002, 50, 3501-3512.

[6] B.X. Liu, W.S. Lai and Q. Zhang, *Mater. Sci. Eng., R*, 2000, 29, 1-48.

[7] I.P. Jain and G. Agarwal, *Surf. Sci. Rep.*, 2011, 66, 77-172.

[8] J.F. Ziegler, J.P. Biersack and U. Littmark, *The Stopping and Range of Ions in Solids*, Pergamon Press, New York, 1985, ch.2, pp.79-82.

[9] D. Turnbull, *Contemp. Phys.*, 1969, 10, 473-483.

[10] Z.P. Lu, H. Tan, Y. Li and S. C. Ng, *Scripta Mater.*, 2000, 42, 667-673.

[11] Z.Y. Suo, K.Q. Qiu, Q.F. Li, J.H. You, Y.L. Ren and Z.Q. Hu, *Mater. Sci. Eng., A*, 2010, 528, 429-433.

[12] A. Inoue, T. Zhang and T. Masumoto, *Mater. Trans. JIM*, 1990, 31,177-183.

[13] M.C. Weinberg, *J. Non-Cryst. Solids*, 1994, 167, 81-84.

[14] K. Mondal and B.S. Murty, *J. Non-Cryst. Solids*, 2005, 351, 1366-1371.

[15] Q. Chen, J. Shen, D. Zhang, H. Fan, J. Sun and D.G. Mccartney, *Mater. Sci. Eng., A*, 2006, 433,155-160.

[16] X.H. Du, J.C. Huang, C.T. Liu and Z.P. Lu, *J. Appl. Phys.*, 2007, 101, 086108.

[17] L. Xia, S.S. Fang, Q. Wang, Y.D. Dong and C.T. Liu, *Appl. Phys. Lett.*, 2006, 88,171905.

[18] L. Xia, W.H. Li, S.S. Fang, B.C. Wei and Y.D. Dong, *J. Appl. Phys.*, 2006, 99, 026103.

[19] F.R. De Boer, R. Boom and W.C. Mattens, *Cohesion in Metals: Transition Metal Alloys*, North-Holland, Amsterdam, 1989, ch. 2, pp. 79-82.

[20] X. Ji, Y. Pan and F. Ni. *Mater. Design*, 2009, 30, 842-845.

[21] A.H. Cai, X. Xiong, Y. Liu, W.K. An, G.J. Zhou, Y. Luo, T.L. Li and X.S. Li, *J. Non-Cryst. Solids*, 2013, 376, 68-75.

[22] T.L. Wang, J.H. Li and B.X. Liu, *Phys. Chem. Chem. Phys.*, 2009, 11, 2371-2373.

[23] N. Li, J.H. Li and B.X. Liu, *RSC Adv.*, 2014, 4, 20616-20619.

[24] Y. Li, S.H. Liang, N. Li, J.H. Li and B.X. Liu, *Mater. Chem. Phys.*, 2013, 141, 960-966.

[25] M.H. Yang, N. Li, J.H. Li and B.X. Liu, *J. Alloys Compd.*, 2014, 606, 7-10.

[26] N. Li, J.H. Li, Y.Y. Wang and B.X. Liu, *Intermetallics*, 2014, 44, 73-76.

[27] N. Li, J.H. Li, J.B. Liu and B.X. Liu, *Appl. Surf. Sci.*, 2014, 290, 495-498.

[28] Y. Li, T.L. Wang, N. Ding, J.B. Liu and B.X. Liu, *Sci. China Tech. Sci.*, 2012, 55, 1-6.

[29] W.C. Wang, H.F. Yan, F. Zeng and B.X. Liu, *Scripta Mater.*, 2007, 57, 583-586.

[30] T.L. Wang, W.C. Wang, J.H. Li and B.X. Liu, *J. Alloys Compd.*, 2010, 493, 154-157.

[31] T.L. Wang, W.T. Huang, W.C. Wang and B.X. Liu, *Mater. Lett.*, 2010, 64, 96-98.

[32] F.S. Santos, C.S. Kiminami, C. Bolfarini, M.F. de Oliveira and W.J. Botta, *J. Alloys Compd.*, 2010, 495, 313-315.

Figure captions:

Fig. 1. (a) The bright field image and (b) SAD pattern of the $Ni_{40}Mo_{20}Ti_{10}Zr_{30}$ multilayered samples after irradiation to a dose of 1×10^{15} Xe^+/cm^2, and (c) the bright field image and (d) SAD pattern of the formed amorphous alloys after the sample was irradiated to the dose of 3×10^{15} Xe^+/cm^2.

Fig. 2. The correlation between the paramter γ^* value and critical ion-dosage D_c of amorphous alloys formed by IBM (a) upon 180 keV, (b) upon 200 keV.

Table 1 Amorphous phases formed in the $Ni_{40}Mo_{20}(Ti_{1-x}Zr_x)_{40}$ multilayered films upon IBM to various doses (Xe^+/cm^2). The gamma values are given in second line.

	$Ni_{40}Mo_{20}Ti_{40}$	$Ni_{40}Mo_{20}Ti_{30}Zr_{10}$	$Ni_{40}Mo_{20}Ti_{20}Zr_{20}$	$Ni_{40}Mo_{20}Ti_{10}Zr_{30}$	$Ni_{40}Mo_{20}Zr_{40}$
γ^*	2.04	2.97	3.08	3.06	2.69
1×10^{15}	A+B	A+B	A+B	A+B	A+B
3×10^{15}	A+B	A	A	A	A+B
5×10^{15}	A+B	A	A	A	A
7×10^{15}	A	A	A	A	A

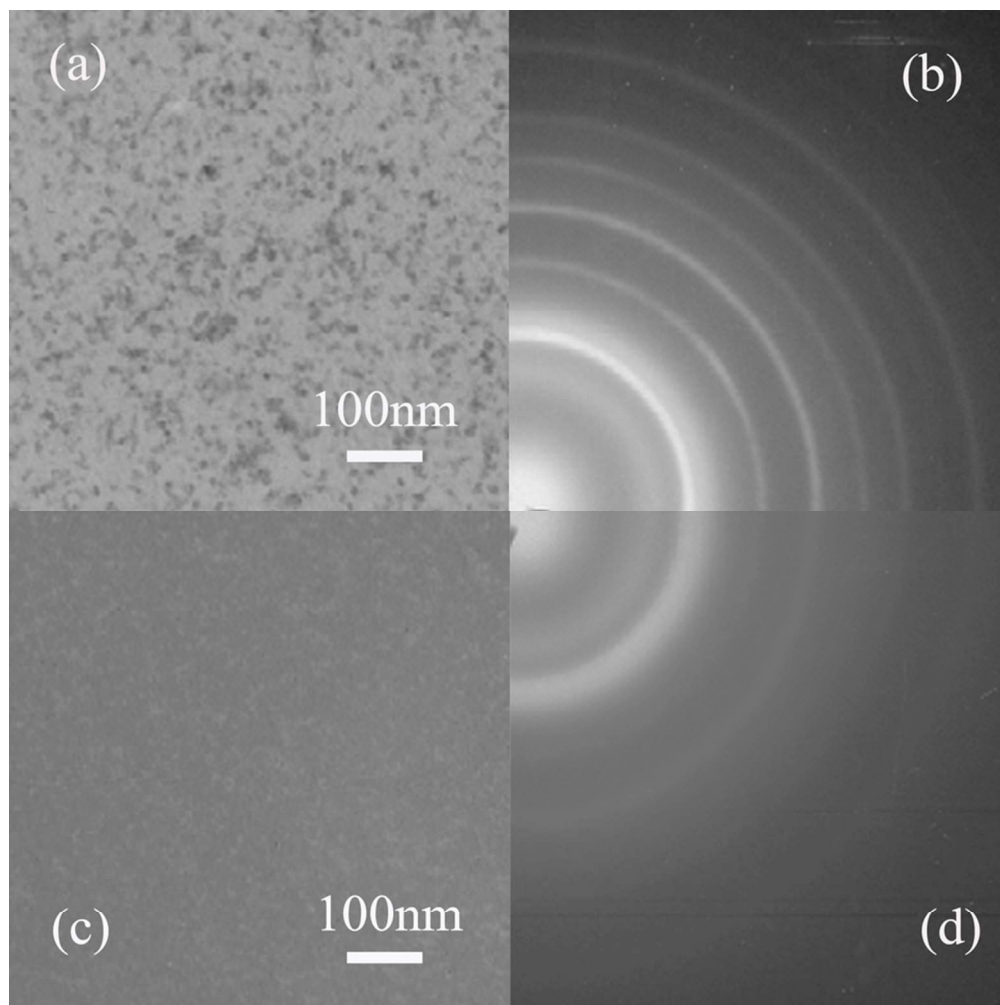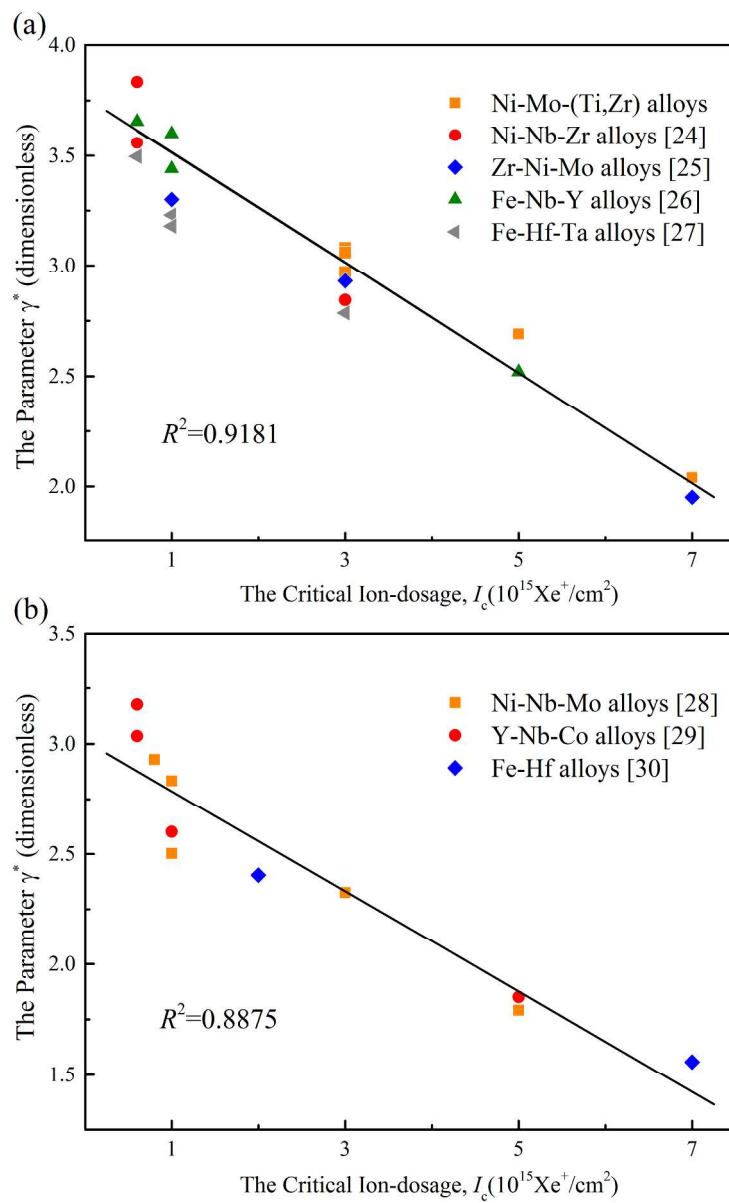A, amorphous phases; B, Mo-based bcc solid solutions.

Figure1
80x80mm (300 x 300 DPI)

(a)

(b)

Figure2
196x321mm (300 x 300 DPI)